International Journal of Research in Engineering and Science (IJRES)
ISSN (Online): 2320-9364, ISSN (Print): 2320-9356
www.ijres.org Volume 4 Issue 3 ǁMarch. 2016 ǁ PP.50-59

A Drain Current Model for Symmetric Double-Gate Polysilicon Thin-Film Transistors

Song Lin Chen
(College of Information Science and Technology, Jinan University, China)

Abstract:- A new analytical solution to the surface potential in symmetric double-gate polysilicon TFTs(DG poly-Si TFTs)is presented,which is single-piece and suitable for a wide range of gate voltages under different conditions. Its high accuracy in predicting the surface potential is verified by a comparison with the numerical results .Furthermore, a drain current model based on terms of surface potential is proposed. Drain current calculations are successfully verified by comparisons with numerical and experimental data.

Keywords:- Poly-si, double-gate,surface potential,drain current

I. INTRODUCTION

Poly-Si TFTs have been receiving a lot of attention due to their advantages for use in high-density active-matrix displays. However, as rules of scaling are approaching the limit, single-gate poly-Si TFTs can't meet the needs of the future because of the short-channel effects.Recently, DG structures of poly-Si TFTs which possess the potential advantages of excellent control of drain-induced-barrier-lowering (DIBL), short-channel effects, larger on/off current ratio, and higher channel conductivity have appeared.

In recent years,several models about DG poly-Si TFTs are presented.A 2D potential distribution model[1]which was was solved by the Greens function approach was proposed. However, it was very complex. The threshold and I – V characteristics of DG poly-Si TFTs[2] were simulated by a 2D simulation tool:Atlas. Its result can serve as a basis for the modeling. In our previous work[3], we developed a drain model for symmetric DG poly-Si TFTs.The drain model in the strong inversion region is adapted from DG MOSFETs.However, their validity is uncertain because they have not been compared with the Pao-Sah model.

In this paper,we develop an accurate surface potential calculation and a drain current model of DG poly-Si TFTs.At first,the surface potential calculation is derived analytically without smoothing function.After that, drain current model of the subthreshold region and above-threshold region has been derived. Finally, the surface potential calculation and drain current model are extensively verified by comparisons with numerical and experimental results.

II. CALCULATION OF THE SURFACE POTENTIAL

The structure of DG poly-Si TFTs is shown in Fig.1,which is an n-channel undoped poly-Si film with a t_{poly}thickness,where $x=\pm t_{poly}/2$ and $x=0$ correspond to the interfaces and the film center, respectively. Herein, this device has two identical gates with the same voltage bias and the top and bottom gate oxides are of equal materials and thicknesses(t_{ox}). The basic assumption we made is that the energy distribution of the traps can be modeled by a constant distribution of deep states and an exponential distribution of tail states.Neglecting the hole concentration, the one-dimensional Poisson equation can be expressed as

$$\frac{\partial^2\varphi}{\partial x^2}=\frac{q}{\varepsilon_{si}}[n_0\exp(\frac{\varphi-V_n}{\phi_t})+N_{deep}+N_{ta0}\exp(\frac{\varphi-V_n}{\phi_g})] \tag{1}$$

Note that $n_0=n_i\exp(E_f/\phi_t q)$, $N_{ta0}=g_{c1}[\pi kT\sin(\pi kT/E_1)]\exp[(E_f-E_c)/E_1]$,and $\phi_g=E_1/q$. Here, q is theelectron charge, ε_{si} is the poly-silicon permittivity,V_n is the channel potential, ϕ_t is thethermalvoltagekT/q, n_i is the intrinsic carrier concentration, E_f is the Fermi-level energy, N_{deep} is the density of deep state ,g_{c1} is the density of acceptor-like tail state , E_1 is the inverse slope of the state, and E_c is the conduction band energy.

Equation (1) must satisfy the following boundary conditions:

$$\left.\frac{d\varphi}{dx}\right|_{x=0}=0 \quad \varphi(0)=\varphi_0 \tag{2}$$

Where φ_0 is the center potential.

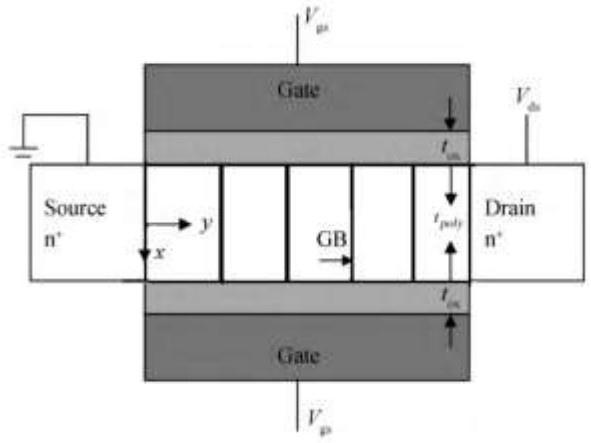

FIG. 1. Diagram of the structure of an undoped DG poly-Si TFT.

Integrating (1) once with the boundary conditions, one obtains

$$E(\varphi,V_n)=\sqrt{\frac{2q}{\varepsilon_{si}}}\left\{\begin{array}{l} n_0\phi_t\left[\exp(\frac{\varphi-V_n}{\phi_t})-\exp(\frac{\varphi_0-V_n}{\phi_t})\right] \\ +N_{deep}(\varphi-\varphi_0)+N_{ta0}\phi_g\left[\exp(\frac{\varphi-V_n}{\phi_g})-\exp(\frac{\varphi_0-V_n}{\phi_g})\right] \end{array}\right\}^{1/2} \tag{3}$$

Using the Gauss' law at the interface, the relation of φ_s and φ_0 with gate bias V_{gs} becomes

$$V_{gs}-V_{fb}-\varphi_s=\frac{\varepsilon_{si}}{C_{ox}}E(\varphi_s,V_n) \tag{4}$$

In order to obtain the solutions of φ_s and φ_0, we split the potential $\varphi(x)$ into four components: the center potential φ_0, the potential $\varphi_1(x)$ contributed by the acceptor-like tail state charge term referenced to φ_0, the potential $\varphi_2(x)$ contributed by the mobile charge term referenced to φ_0. The potential $\varphi_3(x)$ contributed by the deep state charge term referenced to φ_0. So we have

$$\varphi(x)=\varphi_0+\varphi_1(x)+\varphi_2(x)+\varphi_3(x) \tag{5}$$

The expression of $\varphi_1(x),\varphi_2(x)$ and $\varphi_3(x)$ can be obtained by solving the equation

$$\left\{\begin{array}{l} \dfrac{\partial^2\varphi_1}{\partial x^2}=\dfrac{q}{\varepsilon_{si}}\left[N_{ta0}\exp\left(\dfrac{\varphi_1-V_n}{\phi_g}\right)\right] \\ \dfrac{\partial^2\varphi_2}{\partial x^2}=\dfrac{q}{\varepsilon_{si}}\left[n_0\exp\left(\dfrac{\varphi_2-V_n}{\phi_t}\right)\right] \\ \dfrac{\partial^2\varphi_3}{\partial x^2}=\dfrac{q}{\varepsilon_{si}}N_{deep} \end{array}\right. \tag{6}$$

with the following boundary conditions

$$\left\{\begin{array}{l} \varepsilon_{si}\dfrac{\partial\varphi_i(x)}{\partial x}\Big|_{x=0}=0 \\ \varphi_i(x)\big|_{x=0}=0 \end{array}\right. \tag{7}$$

where i=1,2,3.The solutions are

$$\begin{cases} \varphi_1(x) = -2\phi_g \ln\left\{\cos\left[\sqrt{\dfrac{N_{ta0}q}{2\varepsilon_{si}\phi_g}}\exp\left(\dfrac{\varphi_0 - V_n}{2\phi_g}\right)x\right]\right\} \\ \varphi_2(x) = -2\phi_t \ln\left\{\cos\left[\sqrt{\dfrac{n_0 q}{2\varepsilon_{si}\phi_t}}\exp\left(\dfrac{\varphi_0 - V_n}{2\phi_t}\right)x\right]\right\} \\ \varphi_3(x) = \dfrac{qx^2}{2\varepsilon_{si}}N_{deep} \end{cases} \tag{8}$$

Therefore, the surface potential can be written as

$$\begin{aligned} \varphi_s = \varphi\left(\frac{t_{poly}}{2}\right) &= \varphi_0 - 2\phi_g \ln\left\{\cos\left[k_{Nta0}\exp\left(\frac{\varphi_0 - V_n}{2\phi_g}\right)\right]\right\} \\ &- 2\phi_t \ln\left\{\cos\left[k_{Na}\exp\left(\frac{\varphi_0 - V_n}{2\phi_t}\right)\right]\right\} + k_{Nd} \end{aligned} \tag{9}$$

Where $k_{Nde} = \sqrt{\dfrac{n_0 q t_{poly}^2}{8\phi_t\varepsilon_{si}}}$, $k_{Nta0} = \sqrt{\dfrac{N_{ta0}qt_{poly}^2}{8\phi_g\varepsilon_{si}}}$, $k_{Nd} = \dfrac{qt_{poly}^2}{8\varepsilon_{si}}N_{deep}$.

Due to the trapped charge,the surface potential and center potential is less than those in DG MOSEFTS at the same V_{gs}. (9) can't reflect the impact of the reduced of the center potential. Numerical tests also show that φ_s in (9) is less than numerical results when substituting numerical solution φ_0 into (9).Herein,we qualify (9) with two adjusting parameters k_t and k_g as follows to correct the reduced of the center potential.

$$\begin{aligned} \varphi_s = \varphi\left(\frac{t_{poly}}{2}\right) &= \varphi_0 - 2\frac{\phi_g}{k_g}\ln\left\{\cos\left[k_{Nta0}\exp\left(\frac{k_g(\varphi_0 - V_n)}{2\phi_g}\right)\right]\right\} \\ &- 2\frac{\phi_t}{k_t}\ln\left\{\cos\left[k_{Na}\exp\left(\frac{k_t(\varphi_0 - V_n)}{2\phi_t}\right)\right]\right\} + k_{Nd} \end{aligned} \tag{10}$$

To solve k_t and k_g two groups of data must be get. One group is $V_{gf\_max}, \varphi_{s\_max}$ and φ_{0_max}, another is $V_{gf\_turn}, \varphi_{s\_turn}$ and φ_{0_turn}. φ_{s_max} and φ_{0_max} are the surface potential and center potential when $V_{gf} = V_{gs} - V_{fb}$ reach it maximum while φ_{s_turn} and φ_{0_turn} are also the surface potential and center potential when $V_{gf}$is the arbitrary point in the transition region .The first group of data is used to calculate k_t in the strong inversion region while another group of data is used to calculate $k_g$in the transition region.Two groups of data are solved numerically.

The roughly initial guess of $k_g$is given as follows by experience

$$k_g = 1 - \left(\frac{\varphi_{0\_max} - V_n}{\varphi_{0max1} - V_n}\right)\phi_g \tag{11}$$

where $\varphi_{0max1} = V_n - 2\varphi_t \ln\left[\dfrac{t_{poly}}{2L_{di}B}\right]$ is the center potential[7]in the crystalline MOSFETS when V_{gf} reach a maximum .And $B = \arctan[\exp(F)]$ with $F = \left(\dfrac{V_{gf} - V_n}{2\phi_t}\right) - 2\ln\left(\dfrac{2L_{di}}{t_{poly}}\right)$, $L_{di} = \sqrt{\dfrac{2\varepsilon_{si}\phi_t}{qn_0}}$.

Substituting k_{g1}, φ_{s_max} and φ_{0_max} into (10),we can get initial guess of k_t which is denoted as k_{t1}.Then we continue to substitute k_{t1} , φ_{s_turn} and φ_{0_turn} into (10) and substitute above result k_g with φ_{s_max} and φ_{0_max} into (10)again can we finally get k_t.

It should be noted that the combination of (3) and (10) permits an accurate calculation of φ_0 in terms of $V_{gf}$and V_n. However, directly using numerical calculation will results in long computation times and therefore, further simplified calculations are needed. Herein, we try to model φ_0 instead of numerical iteration.The

following expressionsare given as follows[8]

$$\phi_0 = U - \sqrt{U^2 - V_{gf}\phi_{0\max}} \tag{12}$$

$$U = \frac{1}{2}[V_{gf} + (1+r)\phi_{0\max}] \tag{13}$$

Substituting $\phi_{0\max}$, ϕ_{0_turn} and V_{gf_turn} into (12) and (13),r is given by

$$r = \frac{2u_1 - V_{gf\_turn} - \varphi_{0\_\max}}{\varphi_{0\_\max}} \tag{14}$$

Where $u_1 = (\varphi_{0\_turn}^2 + V_{gf\_turn}\varphi_{0\_\max})/(2\varphi_{0\_turn})$.

In order to further improve the accuracy of φ_0,Midpoint Newton's method is used by consisting of (4) and (9) .We use (12) as the initial φ_0.Practical test shows that it requires 1 to 2 external iterations for φ_0 to reach a relative error 1‰. Since φ_0 has been corrected, the final relation between φ_s and V_{gf} is obtained by substituting φ_0 into (10).

III. DRAIN CURRENT MODEL

Accounting for both drift and diffusion current components,the drain current(I_{ds})is given as

$$I_{ds} = -\mu_{eff}\frac{W}{L}\left[\int_{\varphi_{s0}}^{\varphi_{sL}} Q_i d\varphi_s - \phi_t(Q_{iL} - Q_{i0})\right] \tag{15}$$

where μ_{eff} is the effective mobility,W and L are the channel width and length, respectively. φ_{sL} and φ_{s0} are the surface potentials in source and drain ends, respectively. $Q_i = -2\int_{\phi_0}^{\phi_s} n_0 \exp[(\phi - V_n)/\varphi_t]/E(\phi, V_n)d\phi$ is the mobile charge density, Q_{i0} and Q_{iL} are the mobile charge densities at the source and drain ends, respectively. The first term on the right-hand side of (14)is the drift component, and the second is the diffusion component.

In the subthreshold region, Q_i is approximated as follows

$$Q_i = a(V_{gf} - \varphi_s) \tag{16}$$

Where $a = Q_{i0}/(V_{gf} - \varphi_{s0})$.

Substituting (16) into (15),we obtain

$$I_{sub} = \mu_{eff}\frac{W}{L}\left[\frac{a}{2}(\varphi_{s0} - \varphi_{sL})(\varphi_{s0} + \varphi_{sL} - 2V_{gf}) - \phi_t(Q_{iL} - Q_{i0})\right] \tag{17}$$

Herein, $Q_{i0}$and Q_{iL}arecalculate numerically.

In the above-threshold region, Qi is obtained by using Gauss' law at the surface of poly-Si as

$$Q_i = -2C_{ox}(V_{gf} - \varphi_s) - Q_{deep} - Q_t \tag{18}$$

Neglecting the diffusion current component,we substitute (17) into (14) and integrating, the drain current can be obtained as

$$I_{str} = -\mu_{eff}\frac{W}{L}\int_{\varphi_{s0}}^{\varphi_{sL}}[-2C_{ox}(V_{gf} - \varphi_s) - Q_{deep} - Q_t]d\varphi_s \tag{19}$$

Note that we treatQ_{deep} and Q_t in (19)as constants to expediently compute the integral. $Q_{deep}$is written as

$$Q_{deep} = -qN_{deep}t_{si} \tag{20}$$

And Q_t,is approximated as follows according to the mean value theorem for integrals

$$\int_{\varphi_{s0}}^{\varphi_{sL}} Q_t d\varphi_s \approx Q_{t1}(V_a)(\varphi_{sL} - \varphi_{s0}) \tag{21}$$

Where $Q_{tl} = -2\int_{\varphi_{0a}}^{\varphi_{sa}} N_{ta0}\exp[(\varphi - V_a)/\phi_g]/E(\varphi, V_a)d\varphi$ is calculated numerically. φ_{0a} and φ_{sa} are the center potential and surface potential when V_n=V_a.Herein, V_a can be determined as follows according to our numerical analysis

$$V_a = \begin{cases} V_{gs}/2 & V_{gs} < V_{ds} \\ V_{ds}/2 & V_{gs} \geq V_{ds} \end{cases} \tag{22}$$

Now substituting (20) and (21) into (19),we can analytically integrate and get I_{ds}as

$$I_{ab} = \mu_{eff} \frac{W}{L} C_{ox} (\varphi_{s0} - \varphi_{sL})(\varphi_{s0} + \varphi_{sL} - 2V_{gf} - \frac{Q_{deep} + Q_{t1}}{C_{ox}}) \tag{23}$$

The effective mobility is given by[9]

$$\mu_{eff} = \mu_s + \frac{\mu_h \exp\left(\frac{-V_b}{\phi_t}\right)}{1 + \theta_1 V_{gf} + \theta_2 V_{gf}^2} \tag{24}$$

With

$$V_b = \left[(V_{gf} - V_i)^2 + (V_Q - \kappa V_{ds})^2\right]^{1/2} - (V_{gf} - V_i) \tag{25}$$

Where μ_s is the low gate bias mobility, θ_1 and θ_2 are mobility degradation parameters, and κ, V_Q, V_i, μ_h are fitting parameters.

When the channel length is reduced, saturation voltage is smaller than pinch off voltage because of carrier velocity saturation. The difference in saturation voltage can be taken into account by the effective drain voltage V_{dse}. The smooth transition from ohmic to saturation region can be modeled by the following smoothing function[10]

$$V_{dse} = V_{ds} / \{1 + V_{ds} / (\alpha V_{gf})^p\}^{1/p} \tag{26}$$

where parameter p controls the transition from $V_{ds}$to saturation voltage, and here, α is an adjustable parameter which has a channel length L dependence and reduces with deceasing L.

The total drain current is given as

$$I_{ds} = \frac{I_{sub} \times I_{ab}}{(1/I_{sub}^{1/m} + 1/I_{ab}^{1/m})^m} \tag{27}$$

Here, parameter m determines how sharply I_{ds} changes fromthe subthreshold to the above-threshold region.

IV. RESULTS AND DISCUSSIONS

TABLE I. Parameters used for simulation in Fig. 2.

Symbol (units)	Value
t_{poly} (nm)	50
t_{ox}(nm)	100
C_{ox} (F/cm^2)	3.51×10^{-8}
E_1 (eV)	0.06
N_{deep} (cm^{-3})	2×10^{16}
V_{fb} (V)	0
E_f (eV)	0
V_n (V)	0

The results obtained from the proposed model are validated by comparing them with the numerical results in Figs. 2 and 3 from subthreshold to the strong inversion region.The parameters used in the simulation are listed in Tables I and II.The numerical calculations were performed by solving the Poisson equation directly.We can observe from Fig. 2(a) that, $\varphi_0$and $\varphi_s$vary linearly with the gate voltage in the subthreshold region and saturated gradually in the strong inversion region. As g_{c1} increases, φ_s rises much less sharply in the subthreshold region and φ_0 is reduced in all operational region attributed to the higher density of trap states. Fig. 2(b) shows the absolute error of the surface potential approximation. It can be seen that the maximum absolute error is only in the millivolt range. As the increase of V_{gs},the errors decrease.In the strong inversion region,the absolute error is less than 10^{-4} which demonstrates the accuracy of the proposed approximation .The results of (9) as a function of V_{gs} for different V_n are shown in Fig. 3.The total trap charge in the subthreshold region is larger than that in Fig.2.As one can see from Fig. 3 , a good match is achieved between the proposed solutions and numerical results.Fig.4 shows the comparisons between φ_0 predict in our model and that predict in 'finite-difference' method.Comparing with numerical results,we can see that φ_0 inour model is more accurate

than 'finite-difference' method because our model take the impact of the reduced of the center potential into account,which will lead to more accurate surface potential.

The drain current model (27),based on the surface potential,can describe the I-V characteristics when the gate voltage is larger than flat band voltage. In order to support our model,we compare our model with experimental data[4,11,12] and Pao-Sah model on different TFTs.The parameters of TFTs are listed in the simulation are given in Table III.

TABLE II. Parameters used for simulation in Fig. 3.

Symbol (units)	Value
t_{poly} (nm)	50
t_{ox}(nm)	60
C_{ox} (F/cm^2)	3.51×10^{-8}
g_{c1} (cm^{-3}eV^{-1})	2×10^{18}
E_1 (eV)	0.1
N_{deep} (cm^{-3})	1×10^{16}
V_{fb} (V)	0
E_f (eV)	0

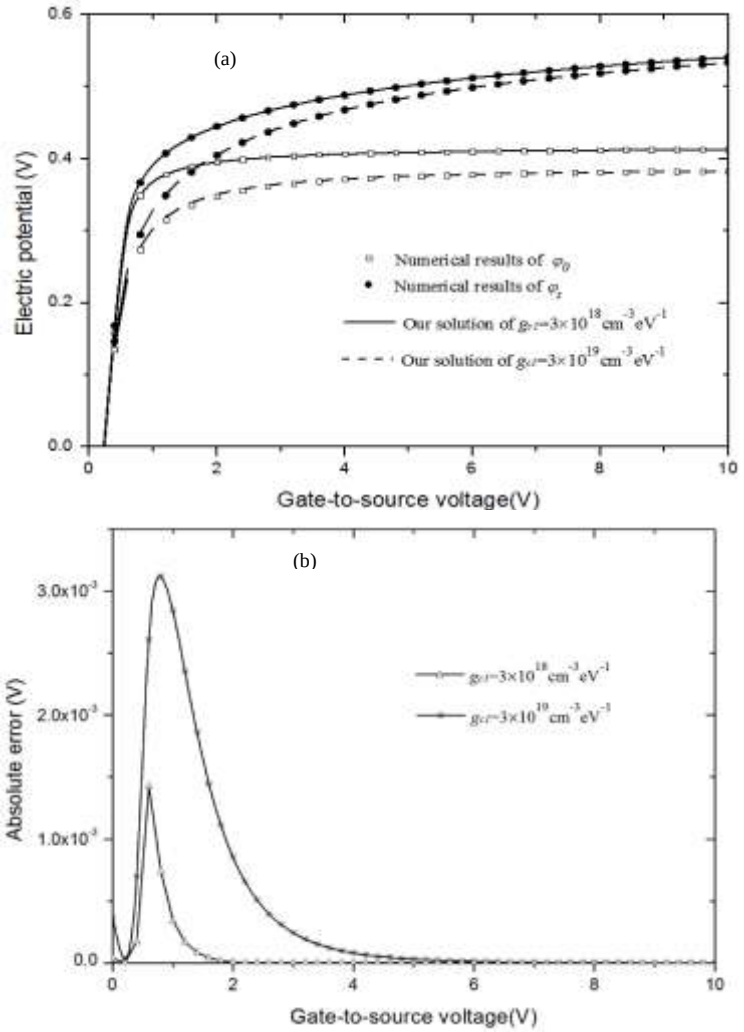

Fig. 2. (a) φ_s and φ_0 with V_{gs} fordifferent g_{c1}(b) Absolute errors of φ_s with V_{gs} fordifferent g_{c1}.

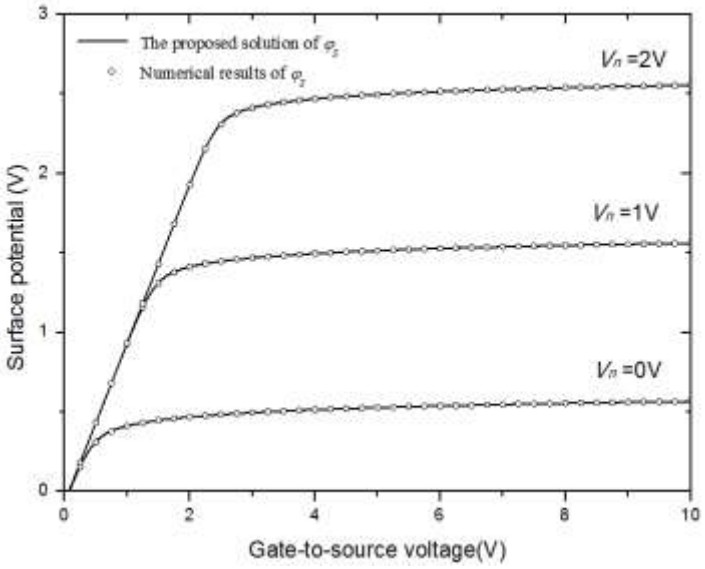

Fig. 3. φ_s with V_{gs} for different channel potentials V_n.

The first validation is shown in Fig. 5(a) and (b). The proposed model reproduces the measured results[4] in a wide range of operation regions.From the Fig.5(a) and (b),It's clear that the behaviors of the short channel devices are well predicted by our model.In addition, good agreement between our model and thePao-Sah model is achieved.

The second validation of the derived model is employed by a comparison with experimental data[12] in Fig. 6(a) and (b).The density of trap states is different from the first validation because of the different fabrication.As we can see, the new model is fairly good in predicting the drain current of the devices and also confirms the accuracy of our model.Moreover,our model and the Pao-Sah model are close.Fig 6(b) shows that the current keep flat after saturation due to the good control of short channel effects of the TFTs.

The third validation is demonstrated in Fig. 7.We can see that the calculated results are in good agreement with thePao-Sah model and measured ones[11] in the sub and above-threshold regions with both logarithmic and linear scales.

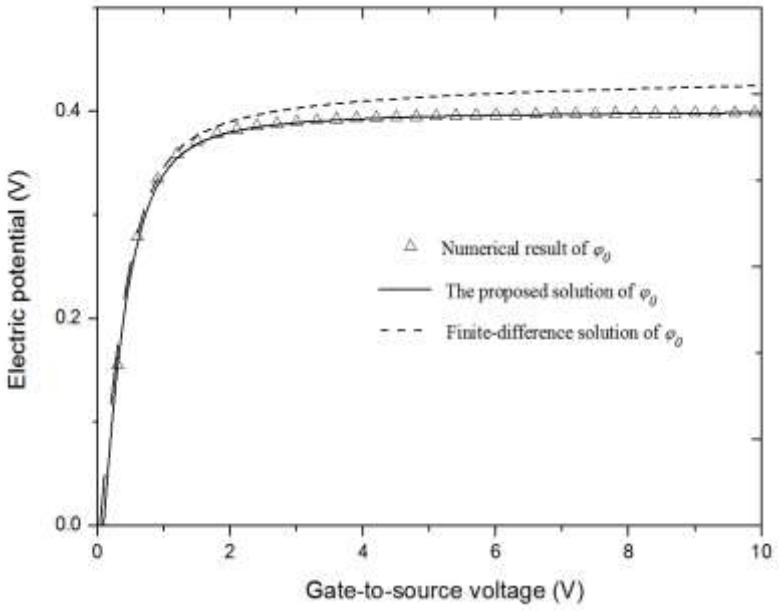

Fig. 4. Comparisons of φ_0 between our model and 'finite-difference' method at V_n=0V.
Parameters used in simulations are still listed in Table II.

TABLE III .Parameters for simulation

Symbol (units)	TFTs in Fig.5	TFTs in Fig.6	TFTs in Fig.7
W(μ m)	1	10	1
L(μ m)	1	10	10
t_{poly} (nm)	100	50	50
t_{ox}(nm)	100	200	90
C_{ox} (F/cm^2)	3.51×10^{-8}	3.51×10^{-8}	3.51×10^{-8}
g_{c1} (cm^{-3}eV^{-1})	2×10^{19}	2×10^{18}	3×10^{18}
E_1 (eV)	0.05	0.08	0.1
N_{deep}(cm^{-3})	2×10^{16}	2×10^{16}	1×10^{16}
V_{fb} (V)	-3	0	-2
E_f (eV)	0	0	0
μ_s (cm^{2}V^{-1}s^{-1})	0	5×10^{-4}	30
μ_h (cm^{2}V^{-1}s^{-1})	310	50	1100
θ_1	1×10^{-3}	1×10^{-3}	1.3×10^{-2}
θ_2	1.5×10^{-3}	2.8×10^{-3}	1.1×10^{-2}
V_Q (V)	0.1	1.2	0.2
κ	0.01	0.01	0.02
V_i (V)	0	1.3	2.6
α	0.16	0.22	-
p	1.5	1.6	-
m	0.06	0.05	0.05

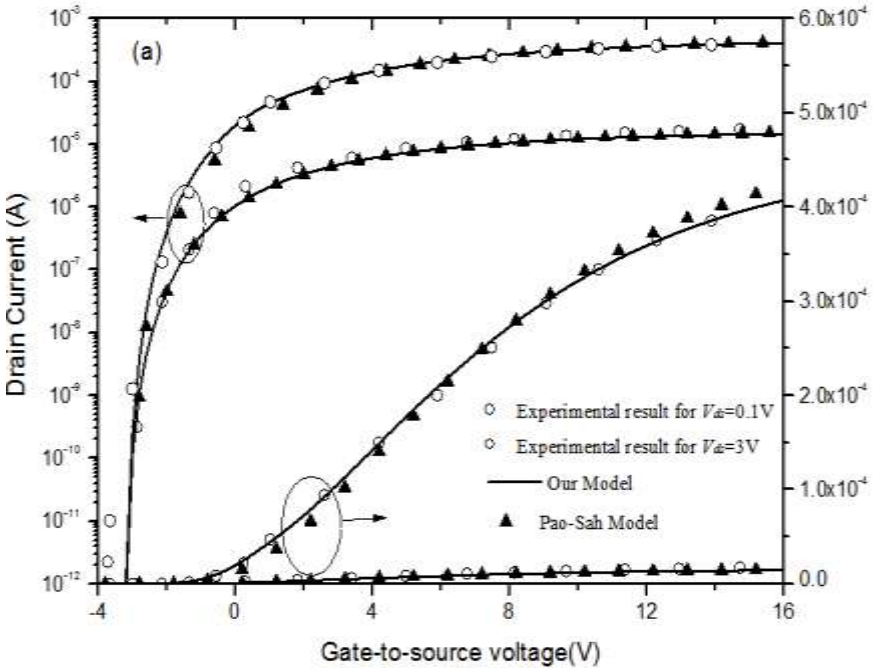

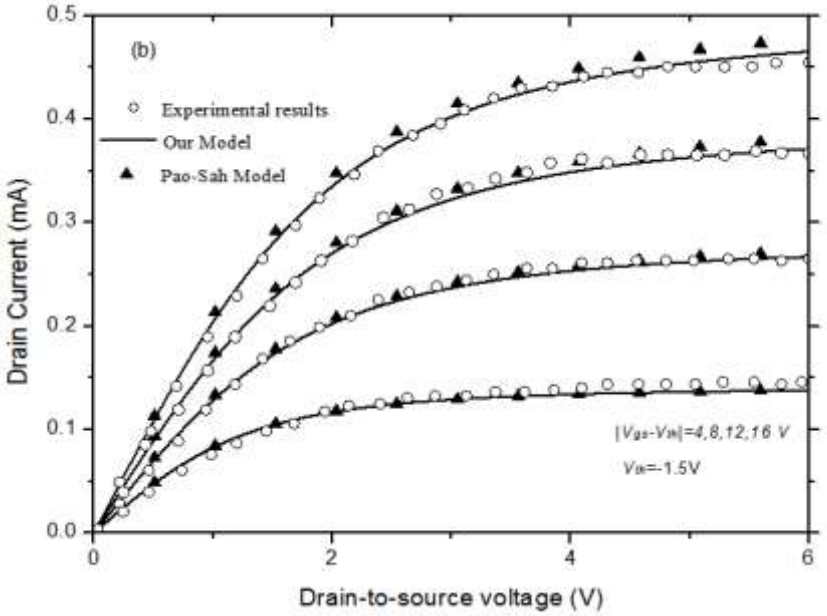

Fig. 5. Comparison between modeled and experimental results[4]for a shortchannel device(W/L is $1\mu m/1\mu m$) with (a) transfer characteristics and (b) output characteristics.

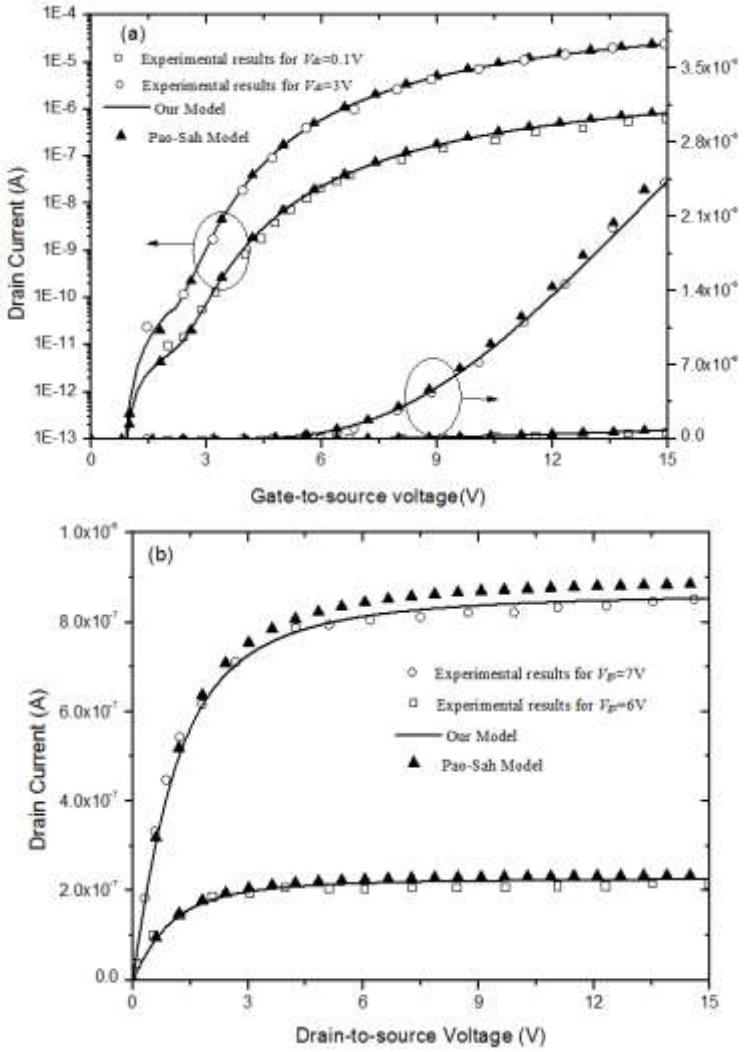

Fig. 6. Comparison between modeled and experimental results[12](W/L is $10\mu m/10\mu m$) with (a) transfer characteristics and (b) output characteristics.

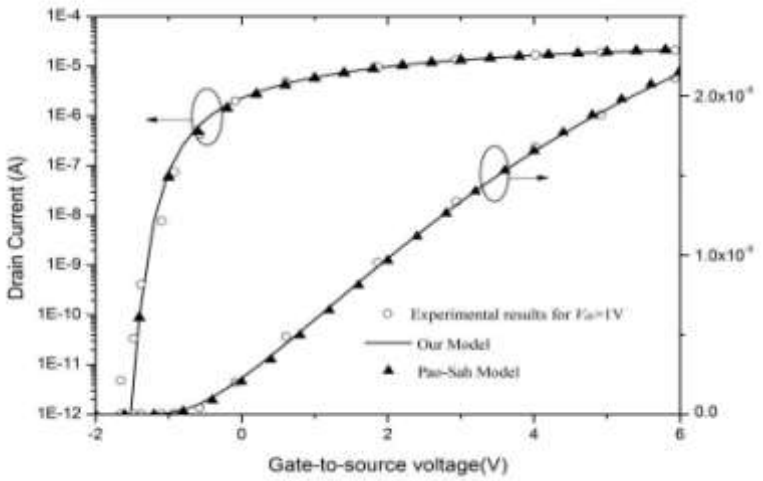

Fig. 7. Comparison between modeled and experimental results[11] (W/L is $1\mu m/10\mu m$)with transfer characteristics

V. CONCLUSION

In this paper, a surface-potential-based drain current model for symmetric undoped or lightly doped DG poly-Si TFTs,valid in a wide range of operational regions is presented.First,the proposed model accounts for monoenergetic deepstate around the midgap and an exponential distribution of DOS near the conduction band edge.Second, an accurate calculation of surface potential and potential at the center of poly-Si layer is done, and the accuracy of the calculation has been verified by the thorough comparisons with numerical iterative results under different conditions. Third, the drain current model,based on the calculated surface potential,is valid in all operation regions above the flatband voltage.The results show that the drain current model of DG poly-Si TFTs is satisfactory for various kinds of devices.

REFERENCE

[1]. Sehgal A, Mangla T, Chopra S, et al. Physics based threshold voltage extraction and simulation for poly-crystalline thin film transistors using a double-gate structure[J]. Semicond Sci Technol,2006, 21(3): 370

[2]. Wang L, Ren Y, Han D, et al. Asynchronous double-gate polycrystalline silicon thin-film transistors for AM-OLED pixel circuits. IEEE 11th International Conference on Solid-State and Integrated Circuit Technology (ICSICT), 2012, DOI: 10.1109/ICSICT.2012.6467841

[3]. Ma Xiaoyu,Deng Wanling and Huang Junkai,Explicit solution of channel potential and drain current model in symmetric doublegate polysilicon TFTs [J].Journal of Semiconductors,2014,35(3).

[4]. Tsai C C, Wei K F, Lee Y J, et al. High-performance shortchannel double-gate lowtemperature polysilicon thin-film transistors using excimer laser crystallization[J]. IEEE Electron Device Lett, 2007, 28(11): 1010

[5]. Zhang S., Han R., Sin J. K. O., et al.A novel self-aligned double-gate TFT technology [J]. IEEE Electron Device Lett.,2001, 22(11): 530-532

[6]. Lin H C, Lin Z M, Chen W C, et al. Read characteristics of independent double-gate poly-Si nanowire SONOS devices[J]. IEEE Trans Electron Devices, 2011, 58(11): 3771

[7]. Bo Yu,, Huaxin Lu, Minjian Liu, and Yuan Taur,Explicit Continuous Models for Double-Gate and Surrounding-Gate MOSFET[J].IEEE TRANSACTIONS ON ELECTRON DEVICES,2007,45(10).

[8]. Ortiz-Conde A, García-Sánchez F J, Muci J, et al. A review of core compact models for undoped double-gate SOI MOSFETs. IEEE Trans Electron Devices, 2007, 54(1): 131.

[9]. Deng W, Zheng X, Chen R. A new poly-Si TFTs DC model for device characterization and circuit simulation[J]. Chinese Journal of Semiconductors, 2007, 28(12): 1916.

[10]. M. D. Jacunski, M. S. Shur, A. A. Owusu, T. Ytterdal, M. Hack, and B. Iñiguez, "A short-channel DC SPICE model for polysilicon thin-film transistors including temperature effects," IEEE Trans. Electron Devices,vol. 46, no. 6, pp. 1146–1157, Jun. 1999.

[11]. Yusuke Shika,Takuro Bessho,Yasunori Okabe,Hiroyuki Ogata,Shinya Kamo,Kuninori Kitahara and Akito Hara,Impact of the Hydrogenation Process on the Performance of Self-Aligned Metal Double-Gate Low-Temperature Polycrystalline-Silicon Thin-Film Transistors[J].Japanese Journal of Applied Physics,2013,52,03BB01.

[12]. Feng-Tso Chien,Chii-Wen Chen, Tien-Chun Lee, Chi-Ling Wang,Ching-Hwa Cheng, Tsung-Kuei Kang, and Hsien-Chin Chiu,A Novel Self-Aligned Double-Channel Polysilicon Thin-Film Transistor[J].IEEE Trans Electron Devices, 2013, 60(2).